J. Membrane Biol. 177, 129–135 (2000)
DOI: 10.1007/s002320001106

The Journal of
Membrane
Biology



# New Molecular Determinant for Inactivation of the Human L-Type $\alpha_{1C}$ $Ca^{2+}$ Channel

**N.M. Soldatov**[1], **S. Zhenochin**[2], **B. AlBanna**[2], **D.R. Abernethy**[1], **M. Morad**[2]
[1]National Institute on Aging, NIH, Gerontology Research Center, Baltimore, MD 21224, USA
[2]Georgetown University Medical Center, Department of Pharmacology, Washington, DC, USA

Received: 14 January 2000/Revised: 20 June 2000

**Abstract.** Molecular cloning of the human fibroblast $Ca^{2+}$ channel pore-forming $\alpha_{1C}$ subunit revealed (Soldatov, 1992. *Proc. Natl. Acad. Sci. USA* **89:**4628-4632) a naturally occurring mutation $g^{2254} \rightarrow a$ that causes the replacement of the conservative alanine for threonine at the position 752 at the cytoplasmic end of transmembrane segment IIS6. Using stably transfected HEK293 cell lines, we have compared electrophysiological properties of the conventional $\alpha_{1C,77}$ human recombinant L-type $Ca^{2+}$ channel with those of its mutated isoform $\alpha_{1C,94}$ containing the A752T replacement. Comparative quantification of steady-state availability of the current carried by $\alpha_{1C,94}$ and $\alpha_{1C,77}$ showed that A752T mutation prevented a large (≈25%) fraction of the current carried by $Ca^{2+}$ or $Ba^{2+}$ from fully inactivating. This mutation, however, did not appear to alter significantly the $Ca^{2+}$-dependence and kinetics of decay of the inactivating fraction of the current or its voltage-dependence. The data suggests that Ala752 at the cytoplasmic end of IIS6 might serve as a molecular determinant of the $Ca^{2+}$ channel inactivation, possibly regulating the voltage-dependence of its availability.

**Key words:** Calcium channel — Inactivation — Mutant — $Ca^{2+}$ overloading

## Introduction

L-type ($\alpha_{1C}$) $Ca^{2+}$ channel plays a critical role in triggering a cascade of intracellular signaling events leading to contraction, secretion and mitogenesis. This function critically depends on the ability of $\alpha_{1C}$ $Ca^{2+}$ channel to provide spatially defined rapid increases in the intracellular $Ca^{2+}$ concentration in response to membrane depolarization. Subsequent $Ca^{2+}$- and voltage-induced inactivation of the current leads to effective closing of the channel, limiting the $Ca^{2+}$ loading of the cell.

The pore-forming $\alpha_{1C}$ subunit of the $Ca^{2+}$ channel is a membrane protein composed of over 2,100 amino acid residues which form four membrane-spanning repetitive motifs (I–IV), flanked by cytosolic short amino- and long carboxyl-terminal tails (Tanabe et al., 1987). Each repetitive motif is composed of 6 putative transmembrane segments (S1–S6). Linkers between S5 and S6 segments (SS1–SS2) in each motif are believed to be embedded into the plasma membrane and contribute to the pore lining by providing Glu carboxylate groups that form the selectivity filter of the channel (Kim et al., 1993; Tang et al., 1993*a;* Yang et al., 1993). Transmembrane segments S4 contain 3–5 positively charged residues and form an essential part of the voltage sensor (Stühmer et al., 1989). The second quarter of the carboxyl-terminal cytoplasmic tail contains $Ca^{2+}$ sensors for $Ca^{2+}$ induced inactivation of the channel (Soldatov et al., 1997, 1998) including that regulated by calmodulin binding (Lee et al., 1999; Peterson et al., 1999; Qin et al., 1999; Zühlke et al., 1999).

Structural interventions that modify the channel inactivation may provide better insight into molecular mechanisms that regulate the channel, and identify possible therapeutic targets. In this respect structure-function studies of naturally occurring mutations that affect $Ca^{2+}$ channel inactivation may be of particular interest. One of such mutations was originally identified by molecular cloning of the human fibroblast L-type $Ca^{2+}$ channel $\alpha_{1C}$ subunit as a single nucleotide conversion $g^{2254} \rightarrow a$ (Soldatov, 1992). This mutation changes the codon for the invariant Ala752 residue located at the cytoplasmic end of the highly conserved transmembrane segment IIS6 and causes its substitution by Thr. In this work we have incorporated the A752T substitution into the conventional $\alpha_{1C,77}$ $Ca^{2+}$ channel and found that this

*Correspondence to:* N.M. Soldatov

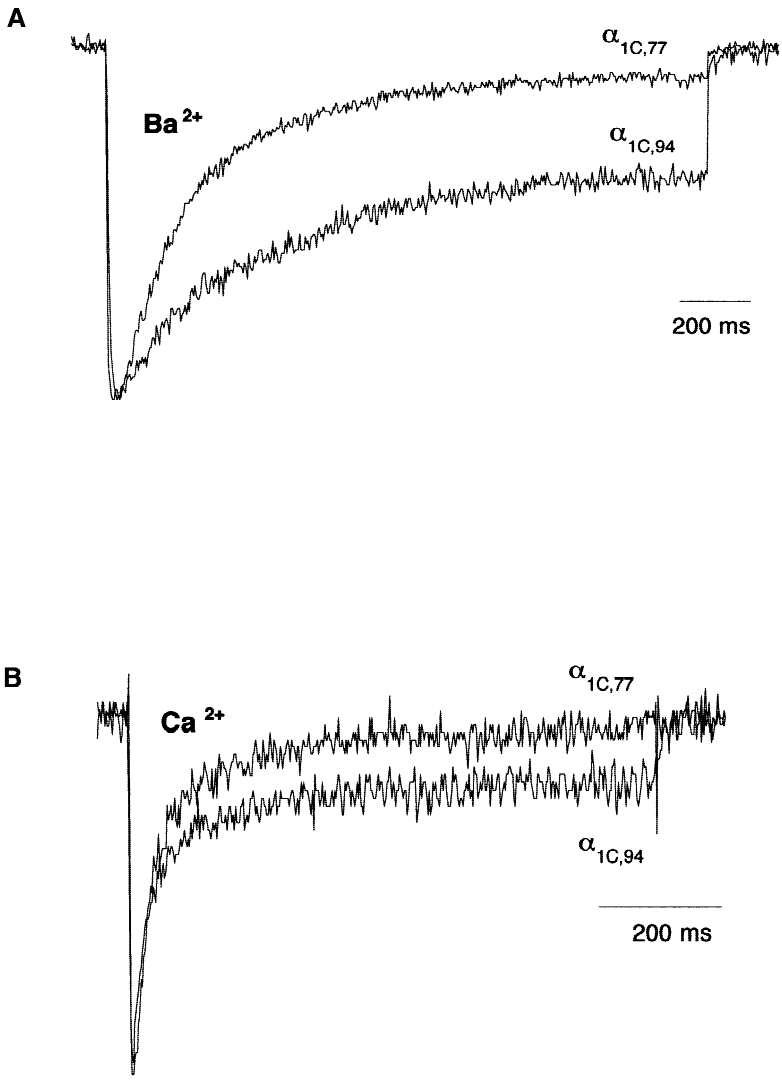


**Fig. 1.** Comparison of time courses of $I_{Ba}$ and $I_{Ca}$ through the $\alpha_{1C,94}$ and $\alpha_{1C,77}$ channels stably expressed in HEK293 cells. Normalized representative current traces were recorded in bath medium containing 20 mM $Ba^{2+}$ (*A*) or 20 mM $Ca^{2+}$ (*B*), in response to test pulses to +10 and +20 mV, respectively. Holding potential ($V_h$) = −80 mV. In the $\alpha_{1C,77}$ channel, the ratio of peak $I_{Ba}$ (444 pA) to $I_{Ca}$ (156 pA) was 2.8 as compared to 4.2 in the $\alpha_{1C,94}$ channel ($I_{Ba}/I_{Ca}$, 570 pA:136 pA).

mutation strongly affects voltage-dependence of the $Ca^{2+}$ channel availability.

## Materials and Methods

### Molecular Biology

All $Ca^{2+}$ channel subunit cDNA constructs used for eukaryotic transfection were prepared in the pcDNA3 vector (Invitrogen, Carlsbad, CA). Kozak sequence (5′-ccgcca-3′) was incorporated at *Hin*d III and *Nco* I (−1) sites of pHLCC77 using the mixture of oligonucleotides 5′-agcttggatccgccac-3′ and 5′-catggtggcggatcca-3′ which were phosphorylated with T4 polynucleotide kinase (New England Biolabs, Beverly, MA) in the presence of 10 mM ATP. The 3′-terminal region was constructed by removing the *Hpa* I (6515)—*Xba* I segment from the 3′-untranslated region and blunt-ends ligation into pHLCC77B. p77cDNA3 was prepared by subcloning the 5′ → 3′ *Hin*d III, *Not* I cassette of pHLCC77B into the pcDNA3 eukaryotic expression vector (Invitrogen).

The *Xmn* I, *Cel* II fragment (open reading frame (ORF), nt 2239–2734) of the cDNA clone f77-2 (Soldatov, 1992) containing $g^{2254}$→a mutation was exchanged with the segment (nt 2239–2734) of pHLCC77 constructed in the pBluescript SK(−) vector (Soldatov, Bouron & Reuter, 1995) leading to pHLCC94. p94cDNA3 was prepared by replacing the *Mun* I (408)/*PpuM* I (2760) fragment of pHLCC77B with the corresponding fragment of pHLCC94 followed by substitution of the *BamH* I, *PpuM* I cassette of the obtained pHLCC94B construct into the p77cDNA3 vector. The p$\alpha_2\delta$cDNA3 construct coding for the auxiliary $\alpha_2\delta$ subunit was prepared by PCR amplification of the $\alpha_2\delta$ ORF with sense 5′-tgccgccatggctgcgggccgcc-3′ and antisense 5′-tcagccatggcagaggcccagc-3′ primers using pCA2 (Singer et al., 1991) as a template, TA-cloning of the PCR product into the pCRII vector (Invitrogen) followed by the subcloning of the *Kpn* I (blunt), *Not* I cassette into the pcDNA3 vector at *Xba* I (blunt), *Not* I sites. The p$\beta_1$cDNA3 construct coding for the auxiliary $\beta_1$ subunit was prepared by PCR amplification of the $\beta_1$ ORF with sense 5′-gccaccatggtccagaagaccag-3′ and antisense 5′-cccccgctacatggcgtgctcc-3′ primers using

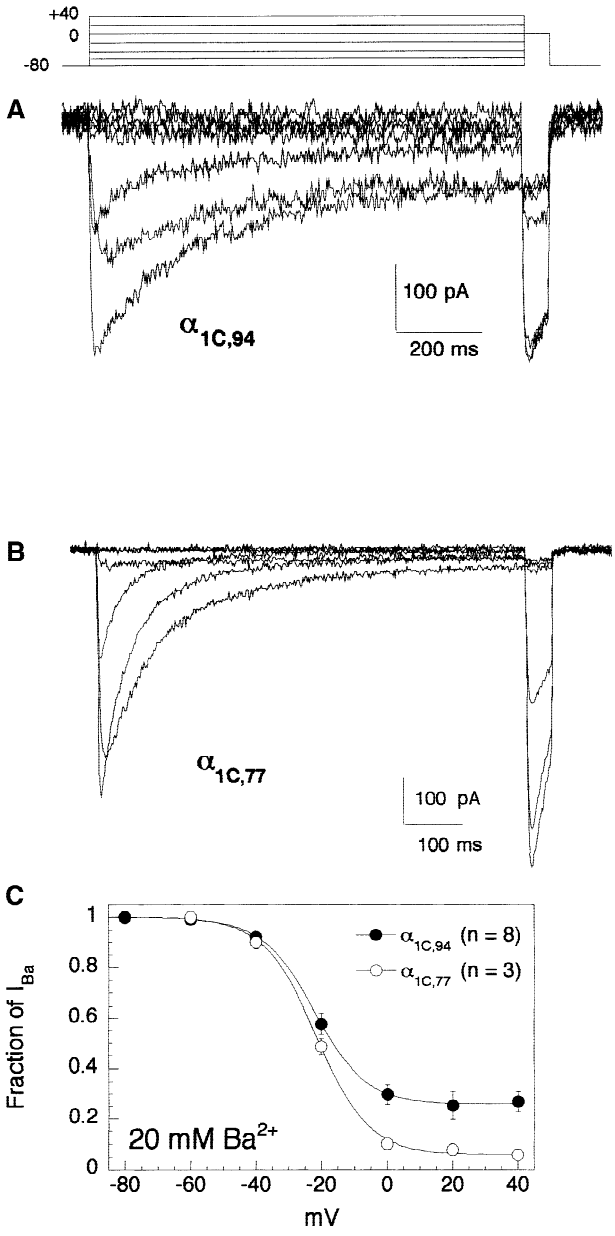


**Fig. 2.** Voltage-dependence of inactivation of $I_{Ba}$ through the $\alpha_{1C,94}$ and $\alpha_{1C,77}$ channels. Representative traces of $I_{Ba}$ through $\alpha_{1C,94}$ (*A*) and $\alpha_{1C,77}$ (*B*) channel recorded in response to conditioning prepulses ranged from −80 to +40 mV (20-mV increments) followed by 50-msec test pulse to 0 mV. The voltage protocol is shown in the upper panel. Duration of the applied conditioning pulses was 0.8 sec ($\alpha_{1C,77}$) and 1.6 sec ($\alpha_{1C,94}$). (*C*) Averaged inactivation curves showing incomplete inactivation of $I_{Ba}$ through $\alpha_{1C,94}$ (●, $n = 8$) as compared to $\alpha_{1C,77}$ (○, $n = 3$). Solid lines represent Boltzmann functions described in Table 1. $V_h = -80$ mV; 20 mM $Ba^{2+}$ in bath medium.

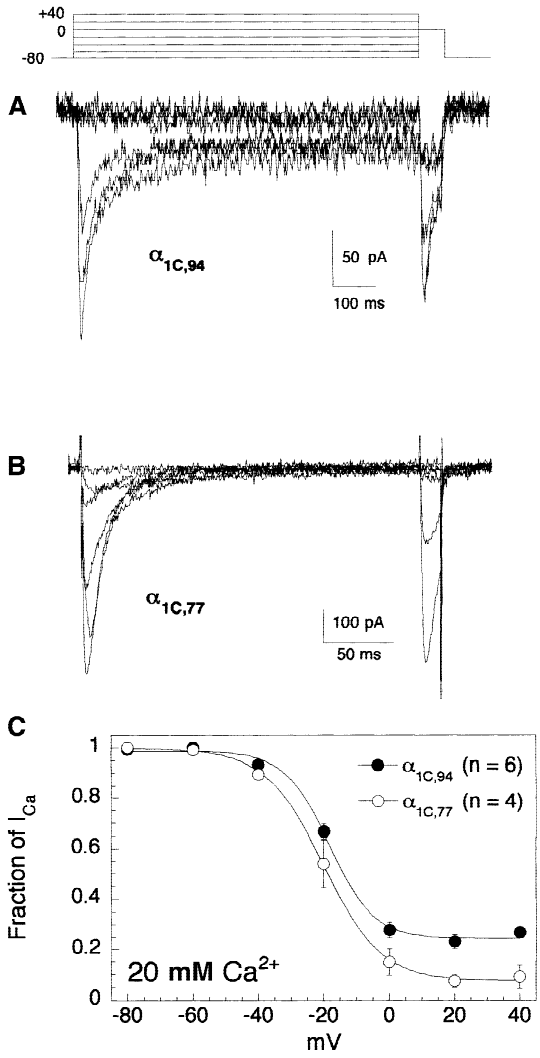


**Fig. 3.** Voltage-dependence of inactivation of $I_{Ca}$ through the $\alpha_{1C,94}$ and $\alpha_{1C,77}$ channels. Representative traces of $I_{Ca}$ through $\alpha_{1C,94}$ (*A*) and $\alpha_{1C,77}$ (*B*) channel recorded in response to conditioning prepulses ranged from −80 to +40 mV (20-mV increments) followed by 15- ($\alpha_{1C,77}$) or 50-msec ($\alpha_{1C,94}$) test pulse to 0 mV. The voltage protocol is shown in the upper panel. Duration of the applied conditioning pulses was 240 msec ($\alpha_{1C,77}$) and 800 msec ($\alpha_{1C,94}$). (*C*) Averaged steady-state inactivation curves showing incomplete inactivation of $I_{Ca}$ through $\alpha_{1C,94}$ (●, $n = 6$) as compared to $\alpha_{1C,77}$ (○, $n = 4$). $V_h = -90$ mV; 20 mM $Ca^{2+}$ in bath medium.

pCaB1 (Mori et al., 1991) as a template, TA-cloning of the PCR product into the pCRII vector (Invitrogen) followed by the subcloning of the *Kpn* I (blunt), *Not* I cassette into the pcDNA3 vector at *Xba* I (blunt), *Not* I sites.

Nucleotide sequences of all PCR products, as well as ligation sites were verified using the ABI Prism™ Dye Terminator Cycle Sequencing Kit with AmpliTaq DNA Polymerase (Perkin-Elmer).

## Expression of $\alpha_{1C,77}$ and $\alpha_{1C,94}$ in HEK293 Cells

Human embryonic kidney 293 cells (HEK293 cells) were grown at 37°C in 5% $CO_2$ in MEM (Gibco-BRL) supplemented with 10% fetal bovine serum, penicillin (100 U/ml), streptomycin (100 μg/ml), and 2 mM L-glutamine (Biofluids, Rockville, MD). Approximately 60% con-

**Table 1.** Influence of A752T mutations of $\alpha_{1C,77}$ to $\alpha_{1C,94}$ on steady-state inactivation

| $\alpha_{1C}$ | Charge carrier | *a* | $V_{0.5}$ | Slope | *n** |
|---|---|---|---|---|---|
| | | % | mV | | |
| 77 | $Ba^{2+}$ | 6.2 ± 1.1 | −21.3 ± 0.6 | 6.9 ± 0.5 | 3 |
| 77 | $Ca^{2+}$ | 7.1 ± 0.8 | −20.2 ± 0.5 | 8.4 ± 0.4 | 5 |
| 94 | $Ba^{2+}$ | 26.8 ± 0.9 | −20.6 ± 0.7 | 8.1 ± 0.6 | 8 |
| 94 | $Ca^{2+}$ | 21.4 ± 0.8 | −18.2 ± 0.5 | 7.1 ± 0.4 | 8 |

Steady-state inactivation curves were measured in stably transfected HEK293 cells in a bath medium containing 20 mM $Ca^{2+}$ or $Ba^{2+}$ using a 2-step voltage clamp protocol (Figs. 2, 3). Conditioning pulses were applied at 10-sec intervals with 10-mV increments up to +60 mV from $V_h = -80$ mV followed by a 100-msec test pulse to 0 mV. Peak current amplitudes were normalized to maximum value. The curves were fitted by a Boltzmann function: $I = a + b/\{1 + \exp[(V - V_{0.5})/k]\}$, where $V$ is the conditioning pulse voltage; $V_{0.5}$ is the voltage at half-maximum of inactivation, *a* and *b* are fractions of noninactivating and inactivating components of the current, respectively, and *k* is a slope factor.
* Number of tested cells.

fluent cultures of HEK293 cells in 35-mm dishes (Corning) were transfected with a total of 4.5 μg DNA sample containing linearized p77cDNA3 or p94cDNA3 mixed with $p\beta_1$cDNA3 and $p\alpha_2\delta$cDNA3 (1:1:1 w/w) using the lipofectamine (Gibco-BRL) method. Recombinant plasmids p77cDNA3, p94cDNA3, and $p\beta_1$cDNA3 were linearized by *Ssp* I, and $p\alpha_2\delta$cDNA3 by *Sca* I. Positive transfectants (20–30 clones) were selected by cultivating for 4 weeks in the presence of G418 (1 mg/ml). Cells expressing $Ca^{2+}$ channel were identified among the positive transfectants directly by the whole cell patch clamp technique.

### *Electrophysiology*

Membrane currents in transfected HEK293 cells were recorded using the whole-cell configuration of the patch-clamp technique (Hamill et al., 1981). The extracellular (bath) solution contained (in mM) 100 NaCl, 20 $BaCl_2$ or $CaCl_2$, 1 $MgCl_2$, 10 glucose, 10 HEPES at pH 7.4. Internal (pipette) solution contained (in mM) 110 CsCl, 5 Mg-ATP, 10 1,2-bis(*o*-aminophenoxy)ethane-N,N,N′,N′-tetraacetate (BAPTA), 20 TEA, 0.2 cAMP, 20 HEPES at pH 7.4. Pipettes (Kimax-51, Kimble). Resistance measured in the bathing solution ranged between 3 and 5 megaohms when the electrode was filled with the internal solution. Series resistance compensation was maximized, and generally ranged around 5–10 megaohms. Current tracings were low pass-filtered at 1 kHz and sampled at 2.5–10 kHz. Data were acquired using pClamp 5.5 software (Axon Instruments, Burlingame, CA), corrected for leakage using an online P/4 subtraction paradigm. Under these conditions, untransfected cells did not show appreciable current.

## Results

### A752T Mutation and the Inactivation of the $\alpha_{1C}$ $Ca^{2+}$ Channel

Fig. 1*A* and *B* shows normalized traces of $I_{Ca}$ and $I_{Ba}$ through the $\alpha_{1C,77}$ and $\alpha_{1C,94}$ channels stably expressed in HEK293 cells. The inactivation of the current through $\alpha_{1C,94}$ was strongly accelerated when extracellular $Ba^{2+}$ was replaced by $Ca^{2+}$, in a manner similar to $\alpha_{1C,77}$. Thus, $\alpha_{1C,94}$ appears to retain the $Ca^{2+}$-induced inactivation property of the $\alpha_{1C,77}$ channel. However, both $I_{Ca}$ and $I_{Ba}$ through the $\alpha_{1C,94}$ channel exhibit notably slower gating kinetics or incomplete inactivation compared to $\alpha_{1C,77}$.

To investigate possible differences in the inactivation of the two channels, we studied the voltage dependence of their availability using $Ba^{2+}$ (Fig. 2) or $Ca^{2+}$ (Fig. 3) as the charge carrier. Variation in the duration of the conditioning prepulse may cause a shift of voltage-dependence of inactivation of the $\alpha_{1C}$ channel without changing its steepness or completeness (Soldatov et al., 1997). Since long depolarizing pulses are poorly tolerated by HEK293 cells expressing the channel, shorter conditioning pulses of 0.8–1.6 sec in $Ba^{2+}$ (Fig. 2*A* and *B*) or 240–800 msec in $Ca^{2+}$ medium (Fig. 3*A* and *B*) were used, because they appeared not to reduce appreciably the fraction of noninactivating component *a* in the $\alpha_{1C,94}$ channel (Table 1). The differences between the wild-type and the mutated channels are illustrated in experiments presented in Figs. 2 and 3. Application of a short test pulses to 0 mV after long conditioning pulses revealed that approximately 25% of the current through the $\alpha_{1C,94}$ channel carried either by $Ba^{2+}$ (Fig. 2*A* and *B*) or by $Ca^{2+}$ (Fig. 3*A* and *B*) did not inactivate (Table 1; Figs. 2*C* and 3*C*). These data suggest that A752T mutation reduced the fraction of channels that inactivate thus affecting the voltage-dependence of availability of the channel.

### A752T Mutation and the Kinetics of Inactivation of the Channel

Comparison of the current traces measured during conditioning pulses shows that $I_{Ba}$ or $I_{Ca}$ through $\alpha_{1C,94}$ inactivated consistently slower than those through the $\alpha_{1C,77}$ channel. This difference may also be due to slowdown of the kinetics of inactivation. To test this possibility, we compared the kinetics of inactivation of $I_{Ca}$ and $I_{Ba}$ through the $\alpha_{1C,94}$ with those through the $\alpha_{1C,77}$ channel at +20 mV. In all cases the time course of the decay of the current was well fit with two exponentials ($\tau_f$ and $\tau_s$, Table 2). Both $Ba^{2+}$-conducting $\alpha_{1C,77}$ and $\alpha_{1C,94}$ channels expressed in HEK293 cells exhibited very large "fast" components of the current ($I_f$) which accounted for 85–90% of the total current. The rapidly decaying component of $I_{Ba}$ through $\alpha_{1C,94}$ inactivated even somewhat faster than those of the $\alpha_{1C,77}$ channel (Table 2). Given that slower inactivating components ($I_s$) of $I_{Ba}$ comprise only 10–15% to the current and have similar $\tau_s$ values in both channels (Table 2), the apparent slower decay of $I_{Ba}$ through $\alpha_{1C,94}$ seen in Fig. 1 may

**Table 2.** Kinetics of $I_{Ba}$ and $I_{Ca}$ decay in $\alpha_{1C,77}$ and $\alpha_{1C,94}$ channels

| $\alpha_{1C}$ | Ion | $\tau_f$ | Fraction of $I_f$ | $\tau_s$ | Fraction of $I_s$ | $n$* |
|---|---|---|---|---|---|---|
| | | msec | % | msec | % | |
| 77 | $Ba^{2+}$ | 56.2 ± 7.4 | 85.5 ± 3.7 | 320.9 ± 72.5 | 14.5 ± 3.7 | 6 |
| 77 | $Ca^{2+}$ | 13.4 ± 0.7 | 95.1 ± 1.4 | 70.3 | 4.9 ± 1.4 | 6 |
| 94 | $Ba^{2+}$ | 34.4 ± 4.8 | 91.2 ± 2.6 | 354 ± 48.8 | 8.8 ± 2.6 | 6 |
| 94 | $Ca^{2+}$ | 22.0 ± 2.5 | 94.9 ± 1.0 | 548 | 5.1 ± 1.0 | 7 |

Inactivation time constants ($\tau$) of $I_{Ba}$ and $I_{Ca}$ were determined from double exponential fitting of current traces elicited by 1-sec test pulses to +20 mV from $V_h = -90$ mV. The fit was obtained by equation: $I(t) = I_\infty + I_f \cdot \exp(-t/\tau_f) + I_s \cdot \exp(-t/\tau_s)$, where $I_\infty$ is the steady-state amplitude of the current, $I$ is the amplitude of the initial current, $f$ and $s$ stand for fast and slow components, respectively.
* Number of cells.

reflect mostly the incomplete inactivation of the mutated channel. A similar conclusion may be reached for the $Ca^{2+}$-conducting channels, as the slower inactivating component of $I_{Ca}$ in both channels contributes to only 5% of the total current.

### Effect of the A752T Mutation on Voltage Sensors of the Channel

Voltage-dependence of inactivation was not significantly changed by the A752T mutation (Table 1). In addition, the voltage dependence of peak currents measured when $Ba^{2+}$ or $Ca^{2+}$ were the charge carriers, was not significantly altered by the A752T mutation (Fig. 4). $I_{Ba}$ through the $\alpha_{1C,94}$ and $\alpha_{1C,77}$ channels had a maximum value around +10 mV (Fig. 4*B*). Replacement of 20 mM $Ba^{2+}$ for 20 mM $Ca^{2+}$ as the charge carrier produced similar rightward shifts of the *I–V* relation in both $\alpha_{1C,77}$ (Fig. 4*A*) and $\alpha_{1C,94}$ (Fig. 4*B*) channels. Thus A752T mutation does not appear to affect significantly the voltage sensors of the channel responsible for peak currents.

To determine the voltage dependence of the noninactivating fraction of the current through the $\alpha_{1C,94}$ channel, we measured the voltage-dependence of the sustained component of $I_{Ba}$ (Fig. 4*C*) and $I_{Ca}$ (Fig. 4*D*) through the $\alpha_{1C,94}$ channel at the end of the 1.6-sec (Fig. 2*A*) and 0.8-sec (Fig. 3*A*) depolarizing pulses, respectively. Both current-voltage relations resembled those measured for the peak currents, but were shifted by 20 ($I_{Ba}$) or 15 mV ($I_{Ca}$) to more negative potentials. However, almost the same shifts were found for $I_{Ba}$ (Fig. 4*C*) and $I_{Ca}$ (Fig. 4*D*) through the $\alpha_{1C,77}$ channel, measured at a time when approximately 75% of the peak current was inactivated. This finding implies that voltage sensors responsible for the activation of the sustained current through the $\alpha_{1C,94}$ channel were not appreciably affected by the A752T mutation, and that the 15–20 mV negative shift of the current-voltage relations (Fig. 4*C* and *D*) may result from the screening effect of the permeating divalent cations.

## Discussion

Human $\alpha_{1C}$ gene is composed of 56 identified exons (Soldatov, 1994), of which 13 exons are subject to alternative splicing. Systematic studies indicate that most the channel splice isoforms exhibit no appreciable differences in the electrophysiological properties in spite of substantial structural changes both at membrane-spanning regions (exons 8/8A, 21/22, 31/32) and cytoplasmic (exons 41A, 44A, 45) or extracellular domains (exons 7, 33) (Soldatov et al., 1995; Bouron, Soldatov & Reuter, 1995; Soldatov et al., 1997; Klöckner et al., 1997; Zühlke et al., 1998). The major finding of the present report is that the single amino acid A752T mutation at the cytoplasmic end of the conserved transmembrane segment IIS6 produces a channel with a large (≈25%) noninactivating component of the current, independent of the charge carrier. The mutation does not significantly alter the $Ca^{2+}$-dependence, voltage-dependence and the gating kinetics of the current.

The nature of the observed $g^{2254}\rightarrow a$ mutation leading to the replacement of the hydrophobic Ala-752 by the hydrophilic Thr residue in IIS6 segment of the $\alpha_{1C}$ channel is not immediately apparent. Two *independent* $\alpha_{1C}$-coding partial cDNA clones bearing this conversion have been identified in nonamplified human fibroblast cDNA library (Soldatov, 1992), thus excluding a possibility of cloning artifact. Since the $g^{2254}\rightarrow a$ conversion in the $\alpha_{1C}$ gene was observed in none of the three different human genomic DNA preparations (Soldatov, 1994), it may represent either a rarely occurring $\alpha_{1C}$ gene mutation or post-translational modification of the transcript.

A752T is a naturally occurring mutation in the human $\alpha_{1C}$ channel, and it may be associated with pathogenesis related to $Ca^{2+}$ overloading, such as brain ischemia, epilepsy or Alzheimer's disease. Interestingly, another hydrophobic to hydrophilic amino acid (V445M) mutation in a very similar position of IS6 segment of the skeletal muscle SCN4A $Na^+$ channel produces a small noninactivating current component and a negative shift in the voltage-dependence of the channel activation, and

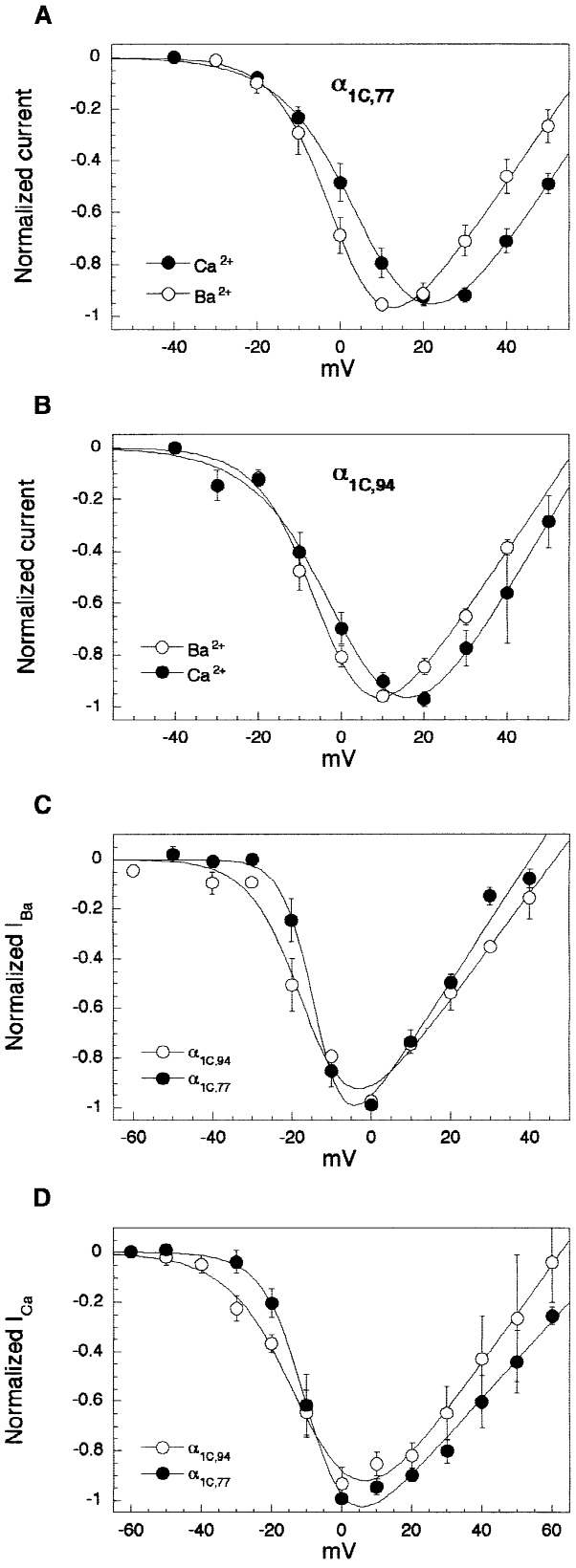


appears to be associated with painful congenital myotonia in humans (Wang et al., 1999).

Our study suggests that alanine-752 of the pore-forming $\alpha_1$ subunit is a structural determinant for the voltage-dependent inactivation of the $Ca^{2+}$ channel. Hydrophobic amino acids in similar positions of transmembrane segments IS6, IIIS6 and IVS6 may also be critical for the channel inactivation. Indeed, previous studies have indicated a role for inactivation of multiple amino acid residues located in or around the transmembrane segments IS6 (Zhang et al., 1994), IIIS5, IIIS6 (Tang et al., 1993*b;* Hering et al., 1997; Berjukow et al., 1999), IVS5 and IVS6 (Motoike et al., 1999). Thus, the voltage-dependent inactivation may, in fact, be regulated by all four repeats as has been previously noted for the other functions of the channel, including ion selectivity (Kim et al., 1993; Tang et al., 1993*a;* Yang et al., 1993) and voltage sensing (Catterall, 1986; Stühmer et al., 1989). Partial (≈25%) loss of the ability to fully inactivate the $\alpha_{1C,94}$ channel may, therefore, be due to incomplete disruption of a voltage-dependent conformational rearrangement in the motif II leading to altered voltage-dependence of the channel availability.

The 15–20 mV negative shift of the current-voltage relation for the sustained current through the $\alpha_{1C,94}$ channel (Fig. 4*C* and *D*) might be largely due to the intracellular screening effect of permeating divalent cations. However, there is some indication that the slope of voltage-dependence of activation of the sustained current through $\alpha_{1C,94}$ is less steeper than that of the $\alpha_{1C,77}$ channel (Fig. 4), suggesting also a possibility that the cooper-

**Fig. 4.** Current-voltage relations for $I_{Ca}$ and $I_{Ba}$ through the $\alpha_{1C,77}$ and $\alpha_{1C,94}$ channels. (*A*) Averaged *I–V* curves for the peak current through the $\alpha_{1C,77}$ channel measured in bath medium containing 20 mM $Ba^{2+}$ (○, $n = 4$) or $Ca^{2+}$ (●, $n = 5$). (*B*) Averaged *I–V* curves for the peak current through the $\alpha_{1C,94}$ channel measured in bath medium containing 20 mM $Ba^{2+}$ (○, $n = 6$) or $Ca^{2+}$ (●, $n = 7$). (*C*) Comparison of averaged *I–V* relations for the steady state $I_{Ba}$ through the $\alpha_{1C,94}$ channel measured at the end of the 1.7-sec conditioning pulses shown in Fig. 3*A* and representing the noninactivating fraction of $I_{Ba}$ (○, $n = 6$) with those through the $\alpha_{1C,77}$ channel (●, $n = 4$) at approximately 200–250 msec after the peak current, where ≈75% of $I_{Ba}$ was inactivated. (*D*) Comparison of averaged *I–V* relations for the slowly inactivating $I_{Ca}$ through the $\alpha_{1C,94}$ channel measured at the end of the 850-msec conditioning pulses shown in Fig. 4*A* and representing "noninactivating" fraction of $I_{Ca}$ (○, $n = 7$) with those through the $\alpha_{1C,77}$ channel (●, $n = 5$) at approximately 30–50 msec after the peak current, where ≈75% of $I_{Ca}$ was inactivated. $V_h = -90$ mV. The curves were fit by the function: $I = Gmax(V - E_{rev})/\{1 + \exp[(V - V_{0.5})/k_{I-V}]\}$, where $E_{rev}$ is reversal potential, $V_{0.5}$–voltage at 50% of the current activation, $k_{I-V}$ – slope factor, and $G_{max}$–maximum conductance.

ativity in the rearrangement of voltage sensors of the channel may be somewhat altered by the A752T mutation. In this respect, similar mutations of transmembrane segments SVI in the other repeats might prove interesting as to whether this site serves as a molecular link between activation and inactivation in $Ca^{2+}$ channel.

This work was supported in part by grant-in-aid of the American Heart Association (Nation's capital Affiliate) and National Institutes of Health grants HL16152 and AG08226. We thank Jee Vang for help in preparation of p94cDNA3, and F. Hofmann and V. Flockerzi (Germany) for gift of clones of $\beta_1$ and $\alpha_2\delta$ subunits. We are grateful to Günter Blobel (Rockefeller University) for the support of the cloning part of this work.

## References

Berjukow, S., Gapp, F., Aczel, S., Sinnegger, M.J., Mitterdorfer, J., Glossmann, H., Hering, S. 1999. Sequence differences between $\alpha_{1C}$ and $\alpha_{1S}$ $Ca^{2+}$ channel subunits reveal structural determinants of a guarded and modulated benzothiazepine receptor. *J. Biol. Chem.* **274:**6154–6160

Bouron, A., Soldatov, N.M., Reuter, H. 1995. The $\beta_1$-subunit is essential for modulation by protein kinase C of an human and a non-human L-type $Ca^{2+}$ channel. *FEBS Lett.* **377:**159–162

Catterall, W.A. 1986. Voltage-dependent gating of sodium channels: correlating structure and function. *Trends Neurosci.* **9:**7–10

Hamill, O.P., Marty, A., Neher, E., Sakmann, B., Sigworth, F.J. 1981. Improved patch-clamp techniques for high-resolution current recording from cells and cell-free membrane patches. *Pfluegers Arch.* **391:**85–100

Hering, S., Aczel, S., Kraus, R.L., Berjukow, S., Striessnig, J., Timin, E.N. 1997. Molecular mechanism of use-dependent calcium channel block by phenylalkylamines: role of inactivation. *Proc. Natl. Acad. Sci. USA* **94:**13323–13328

Kim, M.-S., Morii, T., Sun, L.-X., Imoto, K., Mori, Y. 1993. Structural determinants of ion selectivity in brain calcium channel. *FEBS Lett.* **318:**145–148

Klöckner, U., Mikala, G., Eisfeld, J., Iles, D. E., Strobeck, M., Mershon, J. L., Schwartz, A., Varadi, G. 1997. Properties of three COOH-terminal splice variants of a human cardiac L-type $Ca^{2+}$-channel $\alpha_1$-subunit. *Am. J. Physiol.* **272:**H1372–H1381

Lee, A., Wong, S.T., Gallagher, D., Li, B., Storm, D.R., Scheuer, T., Catterall, W.A. 1999. $Ca^{2+}$/calmodulin binds to and modulates P/Q-type calcium channels. *Nature* **399:**155–159

Mori, Y., Friedrich, T., Kim, M.-S., Mikami, A., Nakai, J., Ruth, P., Bosse, E., Hofmann, F., Flockerzi, V., Furuichi, T., Mikoshiba, K., Imoto, K., Tanabe, T., Numa, S. 1991. Primary structure and functional expression from complementary DNA of a brain calcium channel. *Nature* **350:**398–402

Motoike, H.K., Bodi, I., Nakayama, H., Schwartz, A., Varadi, G. 1999. A region in IVS5 of the human cardiac L-type calcium channel is required for the use-dependent block by phenylalkylamines and benzothiazepines. *J. Biol. Chem.* **274:**9409–9420

Peterson, B.Z., DeMaria, C.D., Adelman, J.P., Yue, D.T. 1999. Calmodulin is the $Ca^{2+}$ sensor for $Ca^{2+}$-dependent inactivation of L-type calcium channels. *Neuron* **22:**549–558

Qin, N., Olcese, R., Bransby, M., Lin, T., Birnbaumer, L. 1999. $Ca^{2+}$-induced inhibition of the cardiac $Ca^{2+}$ channel depends on calmodulin. *Proc. Natl. Acad. Sci. USA* **96:**2435–2438

Singer, D., Biel, M., Lotan, I., Flockerzi, V., Hofmann, F., Dascal, N. 1991. The role of the subunits in the function of the calcium channel. *Science* **253:**1553–1557

Soldatov, N.M. 1992. Molecular diversity of L-type $Ca^{2+}$ channel transcripts in human fibroblasts. *Proc. Natl. Acad. Sci. USA* **89:**4628–4632

Soldatov, N.M. 1994. Genomic structure of human L-type $Ca^{2+}$ channel. *Genomics* **22:**77–87

Soldatov, N.M., Bouron, A., Reuter, H. 1995. Different voltage-dependent inhibition by dihydropyridines of human $Ca^{2+}$ channel splice variants. *J. Biol. Chem.* **270:**10540–10543

Soldatov, N.M., Oz, M., O'Brien, K.A., Abernethy, D.R., Morad, M. 1998. Molecular determinants of L-type $Ca^{2+}$ channel inactivation. Segment exchange analysis of the carboxyl-terminal cytoplasmic motif encoded by exons 40–42 of the human $\alpha_{1C}$ subunit gene. *J. Biol. Chem.* **273:**957–963

Soldatov, N.M., Zühlke, R.D., Bouron, A., Reuter, H. 1997. Molecular structures involved in L-type calcium channel inactivation. Role of the carboxyl-terminal region encoded by exons 40–42 in $\alpha_{1C}$ subunit in the kinetics and $Ca^{2+}$ dependence of inactivation. *J. Biol. Chem.* **272:**3560–3566

Stühmer, W., Conti, F., Suzuki, H., Wang, X., Noda, M., Yahagi, N., Kubo, H., Numa, S. 1989. Structural parts involved in activation and inactivation of the sodium channel. *Nature* **339:**597–603

Tanabe, T., Takeshima, H., Mikami, A., Flockerzi, V., Takahashi, H., Kangawa, K., Kojima, M., Matsuo, H., Hirose, T., Numa, S. 1987. Primary structure of the receptor for calcium channel blockers from skeletal muscle. *Nature* **328:**313–318

Tang, S., Mikala, G., Bahinski, A., Yatani, A., Varadi, G., Schwartz, A. 1993*a*. Molecular localization of ion selectivity sites within the pore of a human L-type cardiac calcium channel. *J. Biol. Chem.* **268:**13026–13029

Tang, S., Yatani, A., Bahinski, A., Mori, Y., Schwartz, A. 1993*b*. Molecular localization of regions in the L-type calcium channel critical for dihydropyridine action. *Neuron* **11:**1013–1021

Wang, D.W., VanDeCarr, D., Ruben, P.C., George, A.L., Jr., Bennett, P.B. 1999. Functional consequences of a domain 1/S6 segment sodium channel mutation associated with painful congenital myotonia. *FEBS Lett.* **448:**231–234

Yang, J., Ellinor, P., Sather, W.A., Zhang, J.-F., Tsien, R.W. 1993. Molecular determinants of $Ca^{2+}$ selectivity and ion permeation in L-type $Ca^{2+}$ channels. *Nature* **366:**158–161

Zhang, J.F., Ellinor, P.T., Aldrich, R.W., Tsien, R.W. 1994. Molecular determinants of voltage-dependent inactivation in calcium channels. *Nature* **372:**97–100

Zühlke, R.D., Bouron, A., Soldatov, N.M., Reuter, H. 1998. $Ca^{2+}$ channel sensitivity towards the blocker isradipine is affected by alternative splicing of the human $\alpha_{1C}$ subunit gene. *FEBS Lett.* **427:**220–224

Zühlke, R.D., Pitt, G.S., Deisseroth, K., Tsien, R.W., Reuter, H. 1999. Calmodulin supports both inactivation and facilitation of L-type calcium channels. *Nature* **399:**159–162